Bcl2L13 is a ceramide synthase inhibitor in glioblastoma

Samuel A. Jensen[a], Andrea E. Calvert[a], Giora Volpert[b], Fotini M. Kouri[a], Lisa A. Hurley[a], Janina P. Luciano[a], Yongfei Wu[a], Alexandra Chalastanis[a], Anthony H. Futerman[b], and Alexander H. Stegh[a,1]

[a]Ken and Ruth Davee Department of Neurology, The Northwestern Brain Tumor Institute, The Robert H. Lurie Comprehensive Cancer Center, Feinberg School of Medicine, Northwestern University, Chicago, IL 60611; and [b]Department of Biological Chemistry, Weizmann Institute of Science, Rehovot 76100, Israel

Edited* by Webster K. Cavenee, Ludwig Institute for Cancer Research, University of California, San Diego, La Jolla, CA, and approved February 28, 2014 (received for review September 4, 2013)

Therapy resistance is a major limitation to the successful treatment of cancer. Here, we identify Bcl2-like 13 (Bcl2L13), an atypical member of the Bcl-2 family, as a therapy susceptibility gene with elevated expression in solid and blood cancers, including glioblastoma (GBM). We demonstrate that mitochondria-associated Bcl2L13 inhibits apoptosis induced by a wide spectrum of chemo- and targeted therapies upstream of Bcl2-associated X protein activation and mitochondrial outer membrane permeabilization in vitro and promotes GBM tumor growth in vivo. Mechanistically, Bcl2L13 binds to proapoptotic ceramide synthases 2 (CerS2) and 6 (CerS6) via a unique C-terminal 250-aa sequence located between its Bcl-2 homology and membrane anchor domains and blocks homo- and heteromeric CerS2/6 complex formation and activity. Correspondingly, CerS2/6 activity and Bcl2L13 abundance are inversely correlated in GBM tumors. Thus, our genetic and functional studies identify Bcl2L13 as a regulator of therapy susceptibility and point to the Bcl2L13–CerS axis as a promising target to enhance responses of therapy-refractory cancers toward conventional and targeted regimens currently in clinical use.

Bcl-2 protein family | intrinsic apoptosis signaling

The sphingolipid ceramide has been widely shown to be an essential component of the mitochondrial phase of apoptosis progression. De novo synthesis of ceramides is catalyzed by six different ceramide synthases (CerS1–6), also referred to as "sphinganine *N*-acyl-transferases," which generate ceramides with distinct fatty-acid chain lengths. Upon apoptosis induction, CerS activity is stimulated at mitochondria and mitochondria-associated membranes (MAMs), a distinct membrane compartment that links the endoplasmic reticulum to mitochondria (1). Ceramide production is necessary for Bcl2-associated X protein (Bax) to insert into the mitochondrial membranes, oligomerize, and subsequently form a pore resulting in mitochondrial outer membrane permeabilization (MOMP) and cytochrome *c* release (2, 3).

Reflecting the important role of ceramide in regulating apoptosis and therapy susceptibility, a role for CerSs in the pathobiology of cancer is beginning to emerge. In breast cancer, CerS2 acts as a proapoptotic protein that increases chemosensitivity and inhibits tumor growth. Consequently, reduced expression of CerS2 has been shown to be a negative prognostic indicator in breast cancer patients (4). Similarly, CerS6 promotes therapy-induced apoptosis in colon cancer cells (5, 6), head and neck squamous cell carcinoma, and lung carcinomas (7, 8), and CerS1 acts as a proapoptotic factor in multiple cancer cell lines (9, 10).

Although it has been well established that CerS-mediated ceramide synthesis is an integral part of mitochondria-controlled intrinsic apoptosis signaling and is an important factor regulating tumorigenesis, specific mechanisms of CerS regulation during apoptosis are not well understood. Here, we have identified and characterized the atypical Bcl-2 family protein Bcl2-like 13 (Bcl2L13) as a CerS inhibitor with elevated expression in glioblastoma (GBM) and other solid and systemic human cancers, and potent tumorigenicity in an orthotopic GBM tumor model. A series of yeast two-hybrid (Y2H), immunoprecipitation, and molecular analyses of intrinsic apoptosis signaling revealed that Bcl2L13 blocks apoptosis in response to conventional and targeted therapy upstream of Bax activation and MOMP, at least in part by inhibiting CerS2 and CerS6 activity. Thus, our genetic and functional studies revealed, for the first time to our knowledge, that CerS activity is under the control of Bcl-2 family proteins and that the Bcl2L13–CerS2/6 signaling axis may represent a novel target to sensitize cancer cells toward extant therapies.

Results

Bcl2L13 Is Overexpressed in Cancer. Bcl2L13 is a Bcl-2 family protein that, similar to canonical members such as Bcl-2 and Bcl-x_L, bears four Bcl-2 homology (BH) motifs (BH1–4) and a hydrophobic C-terminal membrane anchor (MA) (Fig. S1*A*). Unlike classical multi-BH–domain proteins, however, Bcl2L13 possesses a unique C-terminal 250-aa sequence (termed the "BHNo domain") between its BH2 and MA domains, does not heterodimerize with pro- or antiapoptotic Bcl-2 proteins (11), and, as expected, does not cluster with known Bcl-2 proteins as shown by phylogenetic analysis (Fig. S1*B*).

Although initial reports using standard 293T-based transient overexpression systems suggested that Bcl2L13 has a proapoptotic profile (11, 12), recent transcriptomic surveys across multiple malignancies point to putative oncogenic functions of Bcl2L13. Specifically, Bcl2L13 overexpression is associated with

Significance

Molecular mechanisms of therapy (apoptosis) resistance in cancer are poorly understood. Here, we have identified Bcl2-like 13 (Bcl2L13) as a ceramide synthase inhibitor that is overexpressed in glioblastoma (GBM) and other malignancies. Bcl2L13 inhibits therapy-induced apoptosis and promotes GBM tumor growth in vivo. Mechanistically, Bcl2L13 binds to proapoptotic ceramide synthases 2 (CerS2) and 6 (CerS6) and blocks CerS2/6 complex formation and activity. Correspondingly, CerS2/6 activity and Bcl2L13 abundance are inversely correlated in GBM tumors, thereby providing a molecular explanation for the low levels of proapoptotic ceramide species in high-grade gliomas, which are associated with poor survival. To our knowledge, this work provides the first evidence of direct regulation of CerS activity by a Bcl-2 family member and establishes the Bcl2L13–CerS axis as a target for therapeutic intervention.

Author contributions: S.A.J. and A.H.S. designed research; S.A.J., A.E.C., G.V., F.M.K., L.A.H., J.P.L., Y.W., and A.C. performed research; S.A.J., A.E.C., G.V., F.M.K., L.A.H., A.H.F., and A.H.S. analyzed data; and S.A.J., A.H.F., and A.H.S. wrote the paper.

The authors declare no conflict of interest.

*This Direct Submission article had a prearranged editor.

[1]To whom correspondence should be addressed. E-mail: a-stegh@northwestern.edu.

This article contains supporting information online at www.pnas.org/lookup/suppl/doi:10.1073/pnas.1316700111/-/DCSupplemental.

www.pnas.org/cgi/doi/10.1073/pnas.1316700111

chemotherapeutic resistance in childhood acute lymphoblastic leukemia (ALL) and was found to be the only prognostic factor for unfavorable clinical outcome among apoptosis-related genes (13, 14). In addition, Bcl2L13 overexpression drives resistance to ABT-263 in leukemia and small cell lung carcinoma cells and is up-regulated in *ZIC1*-driven liposarcoma (15, 16). In line with these reports, in silico analysis of *Bcl2L13* mRNA expression in solid and systemic cancers confirmed elevated levels of *Bcl2L13* in esophageal adenocarcinoma, oral cavity carcinoma (Fig. S1*C*), anaplastic large cell lymphoma (ALCL), acute myeloid leukemia (AML), and GBM (Fig. 1*A*). Based on the notorious resistance of GBM tumors to extant chemotherapeutic regimens and GBM's highly lethal and progressive course, we focused on GBM as a cancer model for further in-depth studies of Bcl2L13 abundance and function. A series of RT-quantitative PCR (RT-qPCR), Western blot, and immunohistochemistry (IHC) analyses of primary GBM specimens revealed overexpression of Bcl2L13 mRNA and protein in comparison with normal brain. Specifically, we detected highly elevated *Bcl2L13* mRNA levels in the great majority of tumors tested, with two thirds of tumors (23/31) displaying greater than 100-fold increase in Bcl2L13 mRNA in comparison with normal brain (Fig. 1*B*). Although absent in human papillomavirus E6/E7- and telomerase reverse transcriptase (TERT)-immortalized normal human astrocytes and normal brain tissue adjacent to cancerous lesions, Bcl2L13 protein was detected readily in all GBM patient samples by Western blot (Fig. 1*C*) and IHC analyses (Fig. 1*D*; see Fig. 1*E* for quantification of Bcl2L13-postive tumor cells).

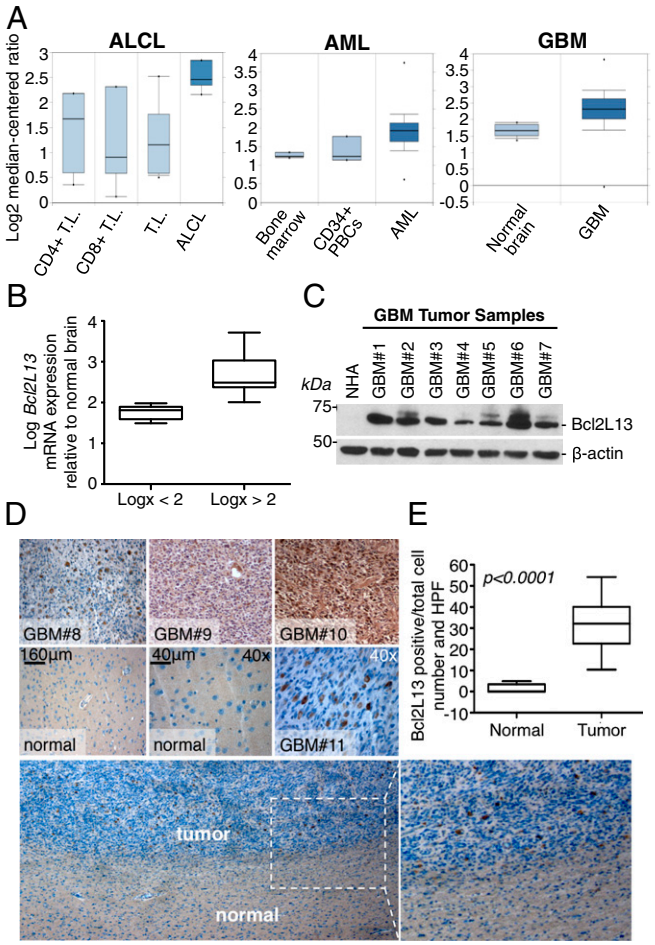

Fig. 1. Bcl2L13 is overexpressed in multiple malignancies, including GBM. (*A*) In silico analysis (www.oncomine.org) of Bcl2L13 expression in solid and systemic malignancies compared with nonmalignant tissue in ALCL [fold change (fc) = 2.36, $P = 3.34 \times 10^{-7}$] (*Left*), AML (fc = 1.51, $P = 1.27 \times 10^{-5}$) (*Center*), and GBM (fc = 1, 58 $P = 5.91 \times 10^{-8}$) (*Right*). PBCs, peripheral blood cells; T.L., T lymphocyte. (*B*) RT-qPCR analysis of *Bcl2L13* expression in 31 GBM tumor samples compared with a pool comprising brain tissue from 23 healthy individuals. Samples are grouped into tumors displaying Bcl2L13 mRNA levels <logx = 2 and >logx = 2 relative to the RNA pooled from 23 healthy individuals. Data are represented as mean ± SD. (*C*) Western blot analysis of Bcl2L13 levels in normal human E6/E7/TERT-immortalized astrocytes (NHA) and multiple GBM tumor samples. β-Actin is shown as a loading control. (*D*) IHC staining for Bcl2L13 in four representative GBM tumor samples and adjacent normal brain. (*E*) Quantification of Bcl2L13-positive cells in normal brain compared with GBM tissue as determined by IHC staining for Bcl2L13. Shown are Bcl2L13-positive cells per total cell number and high-power field (HPF). More than 30 high-power fields were counted. Error bars indicate minimum and maximum values.

Bcl2L13 Inhibits Apoptosis Induced by Conventional and Targeted Therapies. Motivated by these in silico and in situ expression analyses revealing elevated expression of Bcl2L13 in systemic and solid cancers, in particular GBM, and the homology of Bcl2L13 to a family of established apoptosis modulators, we next assessed the role of Bcl2L13 in regulating therapy-induced apoptosis in vitro and tumorigenesis in vivo using cDNA complementation and RNAi-based loss-of-function studies. Lentiviral infection of the glioma cell line SF767 with Bcl2L13-targeting shRNAs (Fig. 2*A*; see Fig. S2 for multiplicity experiments documenting increased caspase activation and annexin V positivity elicited by multiple Bcl2L13-targeting shRNA constructs; hereafter, "shBcl2L13-1" is designated as "shBcl2L13") resulted in a potent increase in postmitochondrial caspase maturation and activity (Fig. 2 *B* and *C*) and amplified phosphatidyl serine translocation (Fig. 2*D*) upon treatment with the pan-kinase inhibitor staurosporine (STS). Conversely, stable overexpression of a *Bcl2L13* cDNA (Fig. 2*E*) blocked caspase activation and activity (Fig. 2 *F* and *G*) and reduced annexin V positivity in response to STS (Fig. 2*H*). Notably, a survey of caspase activation in response to chemo- and targeted GBM therapies [i.e., the EGF receptor (EGFR) and cMet-targeting ATP mimetics erlotinib and SU11274 (Fig. 2*I*) and the diarylheptanoid curcumin (Fig. 2*J*)] confirmed antiapoptotic activity of Bcl2L13. Because Bcl2L13 represents a critical prognostication factor in leukemia (13), we also confirmed the antiapoptotic function of Bcl2L13 in leukemia cells. As in glioma cell lines, Bcl2L13 potently inhibited caspase maturation in STS-treated ALL and chronic myelogenous leukemia cells (CCRF-CEM and K562 cells, respectively), because overexpression of Bcl2L13 blocked caspase activation (Fig. S3*A*). Cells engineered to express Bcl2L13-specific shRNAs stably exhibited increased caspase-3 and caspase-7 activation (Fig. S3*B*), providing evidence that Bcl2L13 is an antiapoptotic factor in multiple types of malignancies. Taken together, this series of reinforcing knockdown and overexpression studies demonstrate that Bcl2L13 acts as a potent inhibitor of conventional and targeted therapy-induced apoptosis in cancer.

Next, the glioma-promoting activity of Bcl2L13 was assessed in in vivo tumorigenesis experiments using SF767 cells with enforced expression of Bcl2L13 and Bcl2L13-targeting shRNAs. Bcl2L13 depletion resulted in impaired GBM progression, and overexpression of Bcl2L13 caused enhanced GBM progression, as measured by the survival of orthotopic xenografts (Fig. 2 *K–M*; $n = 5$; $P = 0.0021$; median survival: shRNA control (shCo) vs. shBcl2L13, 43 vs. 53 d; $n = 5$; $P = 0.0021$; median survival: CSII-vector vs. CSII-Bcl2L13, 59 vs. 51 d).

Bcl2L13 Is a Mitochondrial Protein That Blocks Apoptosis Upstream of Bax Activation and MOMP. To begin to dissect the modus operandi of Bcl2L13, we first determined the subcellular localization of endogenous and epitope-tagged Bcl2L13 species. In agreement with previous studies (11, 17), confocal immunofluorescence and

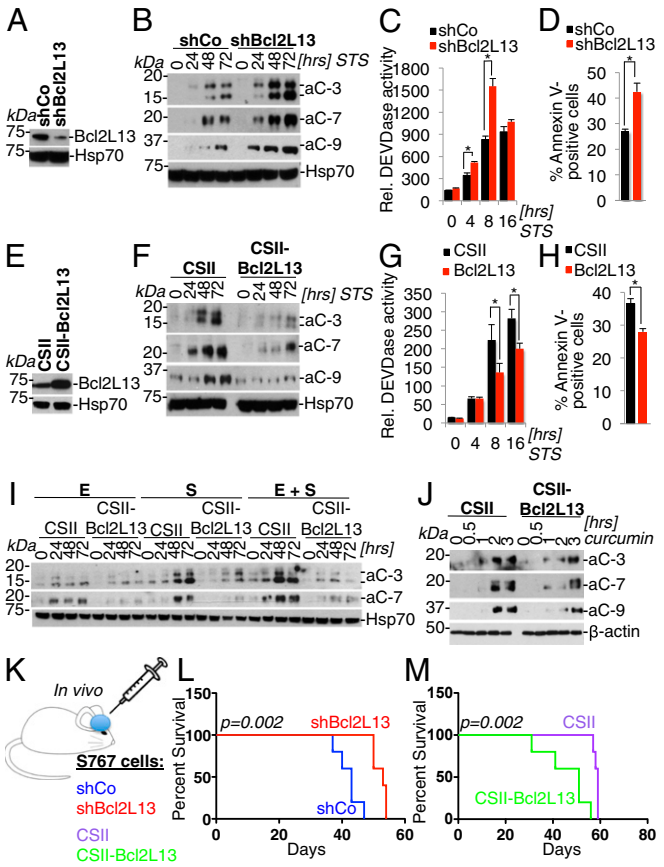

Fig. 2. Bcl2L13 potently inhibits therapy-induced apoptosis and promotes GBM progression in vivo. (*A*) Lentivirus-mediated knockdown of Bcl2L13 using a Bcl2L13-targeting shRNA (shBcl2L13), as assessed by Western blot analysis for endogenous Bcl2L13. Heat shock protein 70 (Hsp70) is shown as a loading control. (*B*) Western blot analysis for active effector caspases in cells with stable knockdown of Bcl2L13 treated with STS (100 nM). aC-3, active caspase-3; aC-7, active caspase-7; aC-9, active caspase-9. (*C*) Quantification by fluorometric DEVDase assay using a fluorochrome-labeled DEVD peptide of effector caspase-3 and -7 activity induced by STS (100 nM). (*D*) FACS-based annexin V quantification of cells harboring shCo and shBcl2L13 following treatment with STS (100 nM) for 24 h. (*E*) Lentivirus-mediated, enforced Bcl2L13 overexpression in SF767 cells. Shown is a Western blot for Bcl2L13; Hsp70 is shown as a loading control. (*F*) Effect of enforced Bcl2L13 expression on STS-induced (100 nM) apoptosis as documented by Western blot analysis for active caspase -3, -7, and -9. (*G*) DEVDase assays of SF767 cells ectopically expressing Bcl2L13. (*H*) FACS-based quantification of annexin V-positive cells following treatment with STS (100 nM) for 24 h. (*I*) Anti-apoptotic activity of enforced Bcl2L13 in SF767 cells upon EGFR and c-Met inhibition by erlotinib (E, 5 μM) and SU11274 (S, 5 μM)], either singly or in combination, as measured by caspase-3 and -7 cleavage. (*J*) Inhibition of curcumin-induced (50 μM) apoptosis by enforced Bcl2L13 expression in SF767 cells as measured by Western blot analysis for active caspase-3, -7, and -9. β-Actin is shown as a loading control. (*K–M*) A GBM xenograft model (*K*) to determine the impact of stable Bcl2L13 knockdown (SF767 cells) (*L*) or Bcl2L13 overexpression (*M*) on GBM progression. Shown are Kaplan–Meier survival curves of xenografts harboring glioma cells with enforced Bcl2L13-targeting shRNA or Bcl2L13 cDNA expression. In *C*, *D*, *G*, and *H*, results are shown as mean ± SD; $^*P < 0.05$.

transmission electron microscopy (TEM) confirmed mitochondrial localization of Bcl2L13 as evidenced by costaining of endogenous Bcl2L13 with the mitochondrial marker cytochrome *c* (Fig. 3*A*) and immunogold labeling of ectopically expressed Bcl2L13 as visualized by TEM (Fig. 3*B*).

The classical Bcl-2–related structural features (i.e., the presence of multiple BH domains and a C-terminal MA, together with exclusive mitochondrial localization and strong inhibition of caspase-9 activation downstream of MOMP) pointed to Bcl2L13 as a factor safeguarding mitochondrial membrane integrity during apoptosis. Thus, as a first step in positioning the actions of Bcl2L13 upstream of, at, or downstream from mitochondria, we assessed the impact of Bcl2L13 overexpression on Bax activation and on the integrity of the outer and inner mitochondrial

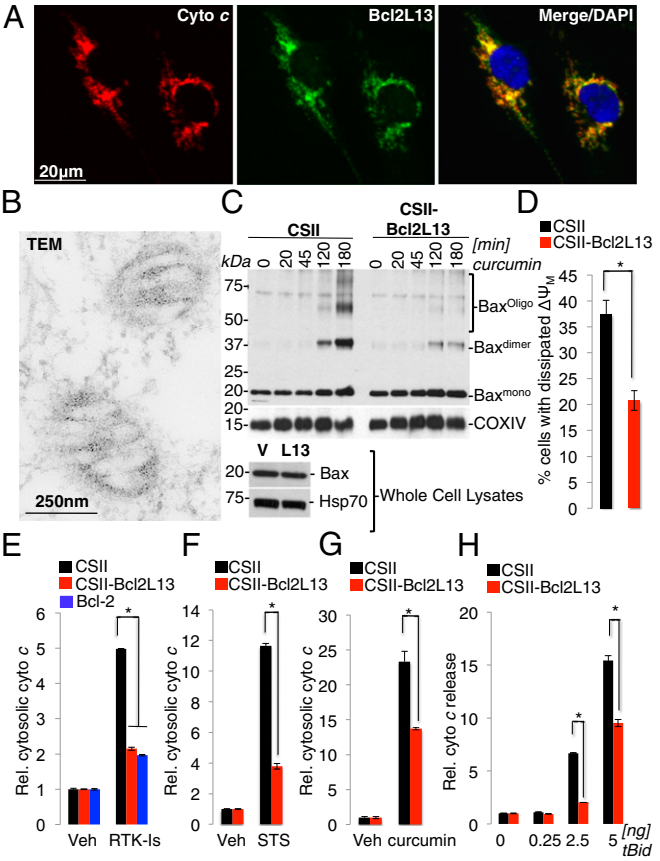

Fig. 3. Bcl2L13 is a mitochondrial protein that inhibits Bax activation and subsequent MOMP and cytochrome *c* release. (*A*) Immunofluorescence staining of LN235 glioma cells using antibodies recognizing endogenous Bcl2L13 and cytochrome *c* (cyto *c*). DAPI is shown as a nuclear counterstain. (*B*) TEM of Bcl2L13-V5–transfected SF767 cells using an anti-V5 antibody in immunogold staining (gold diameter, 10 nm). (*C*) (*Upper*) Western blot analysis for Bax to assess the effect of enforced Bcl2L13 expression on Bax dimerization and the formation of higher-order Bax oligomers upon curcumin-induced (20 μM) apoptosis in SF767 cells. COXIV is used as a mitochondrial loading control. (*Lower*) Anti-Bax Western blot analysis to assess total Bax levels in whole-cell lysates (WCL) in CSII-Bcl2L13 vs. CSII-vector cell lines. (*D*) Effect of Bcl2L13 overexpression on MOMP was determined by analyzing $\Delta\Psi_M$ dissipation in STS-treated (500 nM) Bcl2L13-expressing SF767 cells relative to a vector control. Cells were stained with MitoSense Red, and early apoptotic cells with dissipated $\Delta\Psi_M$ (7-aminoactinomycin D 7–negative/MitoSense Red-positive) were quantified by FACS comparing cells with enforced Bcl2L13 expression with a vector-alone control. (*E*) Control, Bcl2L13-, and Bcl-2–expressing SF767 cells were treated with vehicle (Veh) or the receptor tyrosine kinase inhibitors (RTK-Is) erlotinib (5 μM), SU11274 (5 μM), imatinib (5 μM), AG1024 (5 μM), and KI8751 (2 μM) for 24 h, and cytochrome *c* released from the mitochondria and into the cytosol was assessed by ELISA. (*F* and *G*) Stable SF767 infectants were treated with Veh or STS (100 nM) for 4 h (*F*) and curcumin (200 μM) for 2 h (*G*), and cytochrome *c* release was monitored by ELISA. (*H*) Mitochondria-enriched heavy membrane (HM) fractions isolated from vector control and Bcl2L13-overexpressing SF767 cells were treated with increasing concentrations of recombinant truncated BH3 interacting domain death agonist (tBid). Subsequently, the amount of cytochrome *c* released from HMs was quantified by ELISA. For *D–H*, data are shown as mean ± SD, $^*P < 0.05$.

membrane after exposure to apoptotic stimuli. We demonstrate that Bcl2L13 blocked activation of Bax in SF767 (Fig. 3*C*) and CCRF-CEM cells (Fig. S3*C*; see Fig. S3*D* for quantification of Bax dimerization and membrane insertion), as measured by the extent of Bax oligomerization and insertion into heavy membranes upon induction of apoptosis. In addition, Bcl2L13 inhibited the dissipation of the mitochondrial membrane potential ($\Delta\Psi_M$) in STS-treated cells (Fig. 3*D*) and prevented the release of cytochrome *c* from mitochondria upon treatment of cells with receptor tyrosine kinase inhibitors (Fig. 3*E*) and in response to STS (Fig. 3*F*) and curcumin (Fig. 3*G*). Notably, the inhibition of cytochrome *c* release by Bcl2L13 overexpression was similar in degree to the inhibition by ectopically expressed Bcl-2 (Fig. 3*E*), documenting robust inhibition of the intrinsic apoptosis pathway by Bcl2L13. Together with cell-free assays demonstrating the resistance of isolated mitochondria overexpressing Bcl2L13 to truncated BH3 interacting domain death agonist (tBid)-induced release of cytochrome *c* (Fig. 3*H*), these data show that Bcl2L13 is a mitochondria-associated protein that blocks apoptosis by limiting Bax activation, mitochondrial membrane permeabilization, and subsequent cytochrome *c*-driven caspase activation.

Bcl2L13 Binds to and Inhibits CerS2 and CerS6 Activity. To gain mechanistical insight into the biological function of Bcl2L13, we screened for Bcl2L13–protein interactions using Y2H technology. Our Y2H screen yielded a number of interacting partners (Table S1), most notably CerS2, a member of the ceramide synthase family, which is involved in sphingolipid biogenesis and is responsible for catalyzing the synthesis of ceramide via de novo or recycling pathways. CerS-directed synthesis of ceramide is a critical signaling mechanism during intrinsic apoptosis progression that triggers Bax oligomerization and MOMP (2, 3). In agreement with previous studies (4, 5), we found that CerS2 and CerS6 are proapoptotic enzymes, because overexpression of CerS2 and CerS6 proteins increased STS-induced caspase activation (Fig. S4 *A* and *B*), but knockdown of CerS2 and CerS6 blocked caspase activation in glioma cells (Fig. S4 *C* and *D*). Mirroring the tumor-promoting activities of ectopically expressed Bcl2L13 (Fig. 2 *K–M*), stable knockdown of CerS6 reduced the tumorigenic potential of SF767 as measured by reduced survival of corresponding xenografted mice (Fig. S4 *E* and *F*; $n = 10$; $P < 0.05$; median survival: shCo vs. shCerS6, 39 vs. 35 d). To begin to validate a Bcl2L13–CerS signaling axis, we confirmed the formation of the Bcl2L13–CerS complex by reciprocal coimmunoprecipitations (co-IPs) of Bcl2L13 and CerS2 in glioma cells [Fig. 4*A*, immunoprecipitation (IP) of FLAG-tagged Bcl2L13 followed by Western blot for endogenous CerS2; Fig. 4*B*, IP of FLAG-tagged CerS2 and Western blot for endogenous Bcl2L13].

CerS2 has been shown previously to form heterodimers with other CerS family members, resulting in increased substrate affinity and overall activity (18, 19). Therefore we tested whether Bcl2L13 can bind other CerS members. Similar to CerS2, ectopically expressed Bcl2L13 binds endogenous CerS6 (Fig. 4*C*). Further supporting a Bcl2L13–CerS axis, ectopically expressed Bcl2L13 and CerS2 proteins showed significant colocalization and cocompartmentalization as evidenced by confocal immunofluorescence microcopy (Fig. S5*A*) and submitochondrial fractionation (Fig. S5*B*). Specifically, separation of outer mitochondrial membranes (OMMs), intermitochondrial membrane space (IMS), and inner mitochondrial membranes (IMMs) revealed that Bcl2L13, likely by virtue of its C-terminal MA, is predominantly present in OMMs. As previously reported (20), CerS2 and CerS6 also are found in mitochondrial membranes, most prominently in the outer leaflet. To begin to define the CerS-binding site within the Bcl2L13 polypeptide, we determined that deletion of the BHNo domain (ΔBHNo, Fig. S6*A*) of Bcl2L13 abrogated CerS2 and CerS6 binding to Bcl2L13 (Fig. S6 *B–D*), resulting in a Bcl2L13 polypeptide that failed to block STS-driven caspase

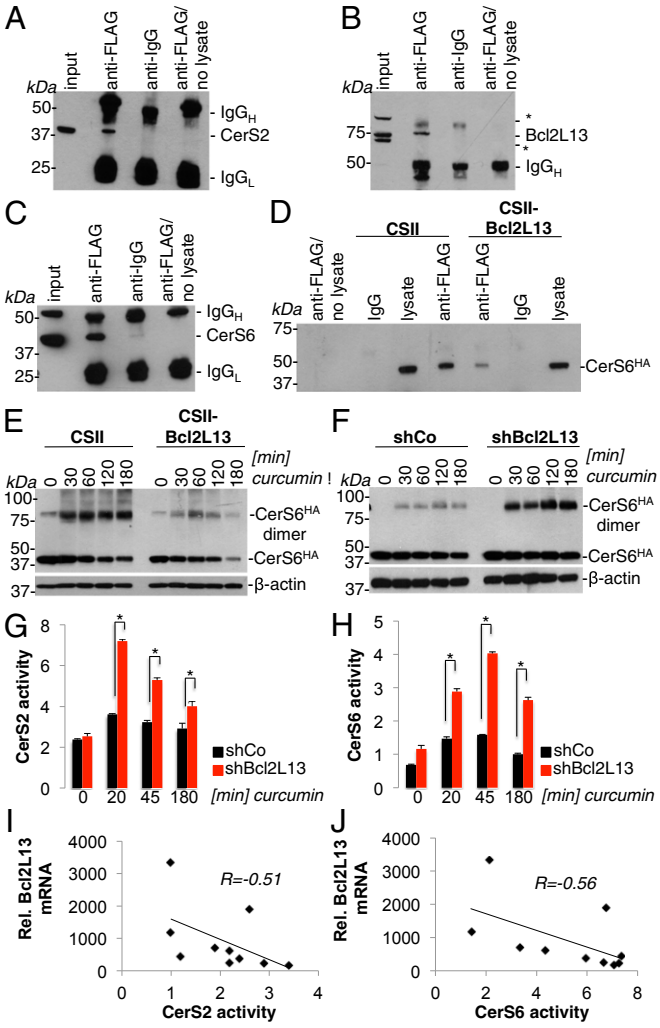

Fig. 4. Bcl2L13 binds to CerS2 and CerS6 and negatively regulates CerS activity. (*A*) Immunoprecipitation of FLAG-tagged Bcl2L13 followed by immunoblotting for endogenous CerS2 in SF767 cells. Migration positions of CerS2 in input and anti-FLAG immunoprecipitates are indicated. (*B*) Immunoprecipitation of FLAG-tagged CerS2 followed by immunoblotting for endogenous Bcl2L13 in SF767 cells. Migration position of endogenous Bcl2L13 is indicated. Asterisks indicate nonspecific background bands. (*C*) Immunoprecipitation of FLAG-Bcl2L13 followed by immunoblotting for endogenous CerS6 in SF767 cells. Migration position of CerS6 is indicated. (*D*) The effect of enforced Bcl2L13 expression on CerS2–CerS6 heteromer formation was assessed by anti-FLAG immunoprecipitation using SF767 cells cotransfected with FLAG-CerS2 and HA-CerS6, followed by immunoblotting with an anti-HA antibody. Migration positions of HA-CerS6 are indicated. (*E*) Effect of enforced Bcl2L13 expression on CerS6 dimerization was determined by treating HA-CerS6–transfected SF767 cells with curcumin (50 μM), followed by Western blot analysis of ectopically expressed HA-CerS6 under nondenaturing conditions. Migration positions of HA-tagged CerS6 monomers and dimers are indicated. β-Actin is shown as a loading control. (*F*) Effect of shRNA-mediated Bcl2L13 KD on CerS6 dimerization was determined by treating HA-CerS6–transfected SF767 cells with curcumin (50 μM) and assessing dimerization of HA-CerS6 under nondenaturing conditions. (*G* and *H*) Effect of Bcl2L13 on CerS2 (*G*) and CerS6 (*H*) enzymatic activity was determined by treating SF767 cells with curcumin (8 μM) for the indicated periods of time before measuring CerS2 or CerS6 activity (as described in *SI Materials and Methods*). Data are shown as mean ± SD, $^*P < 0.05$. (*I* and *J*) Correlation between Bcl2L13 mRNA expression levels and CerS2 (*I*) and CerS6 activity (*J*) in human GBM tumor samples. CerS activity in *G–J* is expressed as pmol (ceramide C16 or C22 species)·min^{-1}·mg^{-1} protein.

activation (Fig. S6 *E–F*). Correspondingly, the canonical Bcl-2 family proteins Bcl-2 and Bcl-x_L, which also are characterized by four BH domains and a MA but lack a BHNo domain, do not form a complex with CerS2 or CerS6 (Fig. S7).

Because homo- and heterodimer formation is required for full CerS activity (19), we assessed the impact of ectopic Bcl2L13 expression on CerS dimerization properties and activity. Bcl2L13 prevented CerS2:CerS6 heteromer formation as assessed by co-IP of tagged CerS proteins in the presence or absence of ectopically expressed Bcl2L13 (Fig. 4*D*). Furthermore, we found that Bcl2L13 potently inhibited CerS6 homodimerization (Fig. 4*E*), and, correspondingly, knockdown of Bcl2L13 increased both dimerization (Fig. 4*F*), and CerS2 and CerS6 activity (Fig. 4 *G* and *H*) in response to curcumin, a known inducer of apoptosis that promotes ceramide production in part through CerS dimerization and activity (19). As expected, a ΔBHNo Bcl2L13 mutant deficient in CerS binding and apoptosis inhibition was unable to inhibit curcumin-induced CerS6 dimerization (Fig. S6*G*).

Finally, by analyzing Bcl2L13 mRNA abundance and CerS activity, we sought to obtain evidence for a Bcl2L13–CerS axis in primary GBM tumor specimens. We uncovered highly significant negative correlations between Bcl2L13 expression and CerS2 and CerS6 activity, further validating our yeast, cell culture, and in vivo xenograft studies (Fig. 4 *I* and *J*). Collectively, these results revealed that Bcl2L13 physically interacted with and inhibited homo-/heterodimerization and activities of CerS2 and CerS6, pointing to ceramide synthesis as an important tumor-suppressive mechanism and confirming that the inhibition of ceramide synthesis is a critical *modus operandi* of antiapoptotic Bcl2L13.

Discussion

In this study, we provide physical and functional evidence that Bcl2L13 acts as an antiapoptotic protein. Bcl2L13 protects mitochondrial membrane integrity upstream of Bax activation by binding to and inhibiting CerS2 and CerS6 activity. Taking these findings together with elevated Bcl2L13 expression in systemic and solid malignancies, including GBM, we propose that Bcl2L13 is an important contributor to therapeutic resistance in cancer and represents a first-in-class Bcl-2 family protein that directly controls CerS biology.

On molecular levels, the presence of multiple BH domains and a C-terminal MA, together with constitutive mitochondrial localization, translate into classical antiapoptotic Bcl-2–like activities, i.e., the protection of outer and inner mitochondrial membrane integrity. Specifically, Bcl2L13 inhibited MOMP, as evidenced by reduced cytochrome *c* translocation into the cytosol and subsequent dissipation of $\Delta\Psi_M$ as an indicator IMM integrity. This profile, coupled with impaired postmitochondrial caspase-9, -3, and -7 activation, is consistent with the ability of Bcl2L13 to block CerS2/6 activity, which in turn can antagonize Bax activation upstream of MOMP. Mechanistically, Bcl2L13 physically binds to CerS2 and CerS6 via its BHNo domain and inhibits homo- and heterodimerization of CerS2 and CerS6. Because the BHNo domain encompasses 250 amino acids of the Bcl2L13 polypeptide, we cannot exclude the possibility that its deletion impacts the 3D structure of Bcl2L13 and thereby alters the binding site for CerS2 and CerS6. Future studies will delineate specific residues within the BHNo required for CerS2/6 interaction. Bcl2L13 also may interact with CerS5, which generates C_{16} ceramide, because all commercial antibodies against CerS6 have been shown to cross-react with CerS5 (18). Importantly, homo- and heteromeric complex formation regulates CerS activity, because substrate binding to one monomer allosterically reduces the substrate K_m for the other monomer (19). This regulation is particularly important for CerS2, which has low-level activity as a monomer but is the main CerS responsible for the generation of very long acyl-chain ceramides (21, 22). Detailed structural analyses and ultimately resolution of the crystal structure of CerSs remain elusive. Consequently, the CerS dimerization interface has not been defined yet. Based on early biochemical studies and in silico 3D structure prediction algorithms, CerSs are transmembrane proteins harboring six transmembrane regions, with two loops facing the lumen of intracellular organelles, such as the IMS (23). The first luminal loop contains a Hox-like domain, and the second luminal loop harbors an LAG1P motif with two conserved histidine residues that are critical for activity and/or substrate binding of CerS. Based on these structural details, we hypothesize that Bcl2L13 anchored in the OMM and facing the IMS binds to the first and/or second luminal loop, thereby preventing the association or provoking the dissociation of CerS homo- and heterodimers (Fig. S8). This mechanism of action represents an effective means of enzyme regulation, because posttranslational regulation occurs rapidly and allows quick adaptation to extrinsic and intrinsic cues to modulate ceramide production and downstream signaling.

Extending beyond its structural role in biomembranes, ceramide has pleiotropic tumor-suppressor functions by virtue of its impact on apoptosis signaling, in particular on the mitochondria-driven intrinsic pathway (24). Multiple studies found that ceramide is required for Bax to permeabilize outer mitochondrial membranes effectively (3, 25). In support of a ceramide–Bax signaling axis, ceramide-rich macrodomains in the outer mitochondrial leaflet are critical for Bax membrane insertion (2). In addition, ceramide-driven increases in intracellular pH can induce conformational changes in Bax and can trigger p38MAPK activation that, together with AKT down-regulation, promotes Bax translocation to mitochondria (17, 26). In line with these studies, we propose that Bcl2L13-mediated inhibition of ceramide production occurs upstream of Bax oligomerization and insertion into mitochondrial membranes, because ectopic Bcl2L13 expression prevented both the formation of high molecular weight Bax complexes and the insertion of Bax into heavy membranes.

Although several studies have suggested that ceramide synthesized in the MAMs traffics to mitochondrial membranes to synergize with Bax (2, 3), additional evidence suggests that purified mitochondria are capable of generating ceramide through either CerS or reverse ceramidase and that CerS activities can be found in OMMs and IMMs (20, 27). We could confirm a mitochondrial localization of CerS2/6 predominantly in the OMMs. Thus we propose that mitochondria-associated Bcl2L13 blocks CerS activity at the level of mitochondrial membranes, thereby lowering ceramide levels in mitochondria membranes and reducing Bax activation, MOMP, and cytochrome *c* release.

Ceramide holds great promise as an antineoplastic agent that can overcome the resistance of cancer cells to therapy by amplifying intrinsic, mitochondria-driven apoptosis progression. However, the rapid clearance of ceramide and the significant adverse side effects of ceramide-generating agents, such as fenretinide, currently being tested in phase I and II clinical trials in lymphomas and solid tumors (28) have limited a wider application of ceramide-based regimens in the clinic. A promising strategy to enhance intracellular ceramide levels involves targeting proteins that regulate ceramide levels. Examples include the acid ceramidase inhibitor DM102 in prostate and breast cancer cell lines (29), tamoxifen (which acts as a potent inhibitor of ceramide glycosylation) in triple-negative breast cancer (24), and, finally, safingol, an inhibitor of sphingosine kinase with efficacies in colon, breast, ovarian, and cervical cancer models currently enrolled in phase I clinical trials (30, 31). Here, we have identified the Bcl-2 family protein Bcl2L13 as a first-in-class inhibitor of CerS activity in cancer, particularly in GBM. Pharmacological inhibition or RNAi-mediated silencing of Bcl2L13 therefore may enable the safe and robust increase of proapoptotic ceramide levels in cancers. Interestingly, a role for ceramide in regulating proliferation, differentiation, and cell death in glioma has begun to emerge. Specifically, in T9 glioma cells nerve growth factor activates sphingomyelin hydrolysis, blocks cellular

proliferation, and induces differentiation (32). In addition, stimulation of primary astrocytes with basic FGF activates sphingomyelin synthase to reduce cellular ceramide levels and promote survival (33). Finally, glioma tumor grade negatively correlates with overall ceramide levels, suggesting that ceramide metabolism may represent a biomarker for GBM progression (35). Taking these findings together, we propose that targeting the Bcl2L13–CerS2/6 interaction represents a promising strategy to restore ceramide production in GBM cells, which in turn lowers the threshold for mitochondrial membrane disintegration and induction of intrinsic apoptosis progression in response to extant conventional and targeted therapeutics.

Materials and Methods

To identify Bcl2L13-interacting proteins, a Y2H screen was performed using the Matchmaker Gold GAL4-Yeast Two-Hybrid system (Clontech Laboratories). Full-length Bcl2L13 was cloned into the bait construct (GAL4 DNA-binding domain-pGBKT7) and was transformed into the *Saccharomyces cerevisiae* Y2HGold strain according to the manufacturer's instructions. The expression of Bcl2L13 in transformed yeast cells was confirmed by Western blot analysis of positive colonies. To assess Bcl2L13–protein interactions, a human fetal brain cDNA library, constructed in the pGADT7-Rec vector and pretransformed into the *S. cerevisiae* Y187 strain, was used as prey for mating. The mated, diploid yeast cells were grown on different stringency-selection media to select for colonies that had bait–prey interactions. The positive colonies were collected and used to amplify the prey insert sequences by PCR using the Matchmaker Insert Check PCR mix (Clontech). The resulting PCR products were separated on an agarose gel, purified using the Gel Extraction kit (Qiagen), sequenced using a T7 primer, and analyzed by BLASTn. A full description of the materials and methods can be found in the *SI Materials and Methods*.

ACKNOWLEDGMENTS. We thank the Cell Imaging Facility, the Flow Cytometry Core Facility, and the Mouse Histology and Phenotyping Laboratory at Northwestern University, all of which are supported by National Cancer Center (NCI) Support Grant P30 CA060553 awarded to the Robert H. Lurie Comprehensive Cancer Center. This research was supported by a grant from the American Cancer Society, Illinois division (to A.H.S.); Israel Science Foundation Grant 0888/11 (to A.H.F.); NCI/National Institutes of Health Training Grant T32CA09560 (to S.A.J. and A.E.C.); the Dixon Translational Research Grants Initiative of the Northwestern Memorial Foundation, the James S. MacDonnell 21st Century Initiative, and the Coffman Charitable Trust (all A.H.S.); The Minerva Foundation (A.H.F.); and the Malkin Scholars Programs of the Robert H. Lurie Comprehensive Cancer Center of Northwestern University (S.A.J.).

1. Stiban J, Caputo L, Colombini M (2008) Ceramide synthesis in the endoplasmic reticulum can permeabilize mitochondria to proapoptotic proteins. *J Lipid Res* 49(3): 625–634.
2. Lee H, et al. (2011) Mitochondrial ceramide-rich macrodomains functionalize Bax upon irradiation. *PLoS ONE* 6(6):e19783.
3. Ganesan V, et al. (2010) Ceramide and activated Bax act synergistically to permeabilize the mitochondrial outer membrane. *Apoptosis* 15(5):553–562.
4. Fan S, et al. (2013) LASS2 enhances chemosensitivity of breast cancer by counteracting acidic tumor microenvironment through inhibiting activity of V-ATPase proton pump. *Oncogene* 32(13):1682–1690.
5. White-Gilbertson S, et al. (2009) Ceramide synthase 6 modulates TRAIL sensitivity and nuclear translocation of active caspase-3 in colon cancer cells. *Oncogene* 28(8):1132–1141.
6. Walker T, et al. (2009) Sorafenib and vorinostat kill colon cancer cells by CD95-dependent and -independent mechanisms. *Mol Pharmacol* 76(2):342–355.
7. Separovic D, et al. (2012) Ceramide synthase 6 knockdown suppresses apoptosis after photodynamic therapy in human head and neck squamous carcinoma cells. *Anticancer Res* 32(3):753–760.
8. Hoeferlin LA, Fekry B, Ogretmen B, Krupenko SA, Krupenko NI (2013) Folate stress induces apoptosis via p53-dependent de novo ceramide synthesis and up-regulation of ceramide synthase 6. *J Biol Chem* 288(18):12880–12890.
9. Senkal CE, et al. (2007) Role of human longevity assurance gene 1 and C18-ceramide in chemotherapy-induced cell death in human head and neck squamous cell carcinomas. *Mol Cancer Ther* 6(2):712–722.
10. Baran Y, et al. (2007) Alterations of ceramide/sphingosine 1-phosphate rheostat involved in the regulation of resistance to imatinib-induced apoptosis in K562 human chronic myeloid leukemia cells. *J Biol Chem* 282(15):10922–10934.
11. Kataoka T, et al. (2001) Bcl-rambo, a novel Bcl-2 homologue that induces apoptosis via its unique C-terminal extension. *J Biol Chem* 276(22):19548–19554.
12. Kim JY, So KJ, Lee S, Park JH (2012) Bcl-rambo induces apoptosis via interaction with the adenine nucleotide translocator. *FEBS Lett* 586(19):3142–3149.
13. Holleman A, et al. (2006) The expression of 70 apoptosis genes in relation to lineage, genetic subtype, cellular drug resistance, and outcome in childhood acute lymphoblastic leukemia. *Blood* 107(2):769–776.
14. Yang YL, et al. (2010) Expression and prognostic significance of the apoptotic genes BCL2L13, Livin, and CASP8AP2 in childhood acute lymphoblastic leukemia. *Leuk Res* 34(1):18–23.
15. Brill E, et al. (2010) ZIC1 overexpression is oncogenic in liposarcoma. *Cancer Res* 70(17):6891–6901.
16. Tahir SK, et al. (2010) Identification of expression signatures predictive of sensitivity to the Bcl-2 family member inhibitor ABT-263 in small cell lung carcinoma and leukemia/lymphoma cell lines. *Mol Cancer Ther* 9(3):545–557.
17. Kim HJ, Oh JE, Kim SW, Chun YJ, Kim MY (2008) Ceramide induces p38 MAPK-dependent apoptosis and Bax translocation via inhibition of Akt in HL-60 cells. *Cancer Lett* 260(1-2):88–95.
18. Mesicek J, et al. (2010) Ceramide synthases 2, 5, and 6 confer distinct roles in radiation-induced apoptosis in HeLa cells. *Cell Signal* 22(9):1300–1307.
19. Laviad EL, Kelly S, Merrill AH, Jr., Futerman AH (2012) Modulation of ceramide synthase activity via dimerization. *J Biol Chem* 287(25):21025–21033.
20. Bionda C, Portoukalian J, Schmitt D, Rodriguez-Lafrasse C, Ardail D (2004) Subcellular compartmentalization of ceramide metabolism: MAM (mitochondria-associated membrane) and/or mitochondria? *Biochem J* 382(Pt 2):527–533.
21. Lahiri S, Futerman AH (2007) The metabolism and function of sphingolipids and glycosphingolipids. *Cell Mol Life Sci* 64(17):2270–2284.
22. Laviad EL, et al. (2008) Characterization of ceramide synthase 2: Tissue distribution, substrate specificity, and inhibition by sphingosine 1-phosphate. *J Biol Chem* 283(9): 5677–5684.
23. Stiban J, Tidhar R, Futerman AH (2010) Ceramide synthases: Roles in cell physiology and signaling. *Adv Exp Med Biol* 688:60–71.
24. Morad SAF, et al. (2013) Tamoxifen magnifies therapeutic impact of ceramide in human colorectal cancer cells independent of p53. *Biochem Pharmacol* 85(8): 1057–1065.
25. von Haefen C, et al. (2002) Ceramide induces mitochondrial activation and apoptosis via a Bax-dependent pathway in human carcinoma cells. *Oncogene* 21(25):4009–4019.
26. Kong JY, Klassen SS, Rabkin SW (2005) Ceramide activates a mitochondrial p38 mitogen-activated protein kinase: A potential mechanism for loss of mitochondrial transmembrane potential and apoptosis. *Mol Cell Biochem* 278(1-2):39–51.
27. Novgorodov SA, et al. (2011) Developmentally regulated ceramide synthase 6 increases mitochondrial Ca2+ loading capacity and promotes apoptosis. *J Biol Chem* 286(6):4644–4658.
28. Kummar S, et al. (2011) Phase I trial of fenretinide lym-x-sorb oral powder in adults with solid tumors and lymphomas. *Anticancer Res* 31(3):961–966.
29. Gouazé-Andersson V, et al. (2011) Inhibition of acid ceramidase by a 2-substituted aminoethanol amide synergistically sensitizes prostate cancer cells to N-(4-hydroxyphenyl) retinamide. *Prostate* 71(10):1064–1073.
30. Ling LU, Lin HM, Tan KB, Chiu GNC (2009) The role of protein kinase C in the synergistic interaction of safingol and irinotecan in colon cancer cells. *Int J Oncol* 35(6): 1463–1471.
31. Ling LU, Tan KB, Chiu GNC (2011) Role of reactive oxygen species in the synergistic cytotoxicity of safingol-based combination regimens with conventional chemotherapeutics. *Oncol Lett* 2(5):905–910.
32. Dobrowsky RT, Werner MH, Castellino AM, Chao MV, Hannun YA (1994) Activation of the sphingomyelin cycle through the low-affinity neurotrophin receptor. *Science* 265(5178):1596–1599.
33. Riboni L, Viani P, Bassi R, Stabilini A, Tettamanti G (2000) Biomodulatory role of ceramide in basic fibroblast growth factor-induced proliferation of cerebellar astrocytes in primary culture. *Glia* 32(2):137–145.
34. Riboni L, et al. (2002) Ceramide levels are inversely associated with malignant progression of human glial tumors. *Glia* 39(2):105–113.